

Radii of Gyration and Screening Lengths of Polystyrene in Toluene as a Function of Concentration

J. S. King* and W. Boyer

Department of Nuclear Engineering, The University of Michigan, Ann Arbor, Michigan 48109

G. D. Wignall

Oak Ridge National Laboratory, Oak Ridge, Tennessee 37830

Robert Ullman

Ford Motor Company, Research Staff, Dearborn, Michigan 48121. Received July 2, 1984

ABSTRACT: Small-angle neutron scattering (SANS) experiments on solutions of polystyrene (PSH) and its deuterated homologue (PSD) in deuterated toluene have been performed over a wide range of concentration. Several redundant measurements demonstrated that the high-concentration technique of extracting single-chain scattering functions is highly reliable. Radii of gyration and screening lengths were fitted to power laws and were found to be $R_g^2 \sim c^{-0.156}$ and $\xi \sim c^{-0.70}$. The results differ significantly from predictions by scaling theory, though the dependence of ξ on c is in good accord with that previously found by other researchers. These experiments were also analyzed by using recent theoretical results of Muthukumar and Edwards. Measurements at different concentrations yielded a reasonably consistent value of the excluded volume interaction parameter.

Introduction

The swelling of macromolecules in a good solvent arises from excluded volume interactions between pairs of monomer units on a single polymer molecule. As the polymer concentration increases, the excluded volume effect is screened and diminishes, and in the limit of bulk polymer the global conformation of a single chain can be described as an unbiased random walk.¹⁻³

It has been an interesting and fruitful endeavor to predict on theoretical grounds how polymer dimensions change in solution as a function of concentration. A number of studies have been published dealing with this problem,⁴⁻⁷ and it is likely that further improvements in the theory will be forthcoming. However, to our knowledge, only one systematic experimental study on the polymer dimension as a function of concentration has been presented.^{4,8} Because of the paucity of data, and the central position of excluded volume interactions in polymer solution behavior, we have undertaken a parallel investigation. This was motivated in part also by our expectation that the dimensions of polymer molecules of modest molecular weight should not obey a concentration law truly applicable only to the asymptotic regime.

Polystyrene in toluene was chosen as the experimental system. The choice was made in part to provide a close parallel with the polystyrene-CS₂ solution experiments of Daoud et al.⁴ In addition, polystyrene in toluene has been widely studied in other contexts, and considerable collateral information is available in the published literature.

Single-chain dimensions of polymer molecules in semidilute or concentrated solutions can be determined in small-angle neutron scattering (SANS) experiments. This has heretofore required extensive measurements on many samples containing trace (~1.0%) concentrations of labeled (deuterated) polymer molecules. We have, instead, taken advantage of the high-concentration method originally reported by Williams et al.⁹ and developed by Summerfield, Akcasu, and other authors.¹⁰⁻¹³ The method reduces the number of samples required and greatly increases the signal/noise ratio. The latter is particularly important in this experiment because the variation of molecular size with concentration is small, and a reliable determination is sensitive to experimental error.

The high-concentration method has been applied to the study of molecular dimensions in bulk polymer by Tangari

et al.¹⁴ and by Wignall et al.¹⁵ These data give no reason to doubt the correctness of the method, but in the bulk the total scattering component, $[S_c(q)]$ of eq 1c is vanishingly small. In solutions this term is large at low concentrations. Consequently, it has been one of our goals here to test rigorously the numerical precision of the method when applied to polymer solutions.

Accordingly this investigation was divided into two parts. In the first, a series of redundant experiments on polystyrene-toluene solutions was undertaken to determine the limits of reproducibility to be assigned to high-concentration labeling when the labeling fraction is varied. For this purpose a series of samples was measured at two different total polymer concentrations (8% and 22%). At each of these concentrations, six samples were prepared with different labeled fractions, varying from zero to unity. The molecular dimensions obtained from each set of six samples should be identical and thus provide a highly redundant set for comparison.

These measurements gave conclusive evidence that the high-concentration method does yield highly reproducible results. The second and main part of the study was subsequently undertaken. Sample solutions were prepared for 11 different total polymer concentrations varying from 2% (mole fraction of monomer) to 100%. For each concentration three different labeled fractions were used to give an element of redundancy to the measurements. To further ensure the reproducibility and eliminate some experimental anomalies encountered during an initial visit to the ORNL spectrometer, a second set of samples was prepared duplicating most of the original concentrations, and measurements were repeated during a second visit. Except for three samples exhibiting anomalous behavior, the data from all these samples were used to determine the concentration dependence of both the radius of gyration and the screening length.

Scattering Equations

The coherent differential scattering cross section of each solution is proportional to the detected count rate, after proper corrections for background and transmission have been made. The cross section is described as the sum of coherent elastic interactions with all chain monomers and all solvent molecules, each treated as a single scattering center. We make the assumption that the solutions are,

Table I
Molecular Weights and Molecular Weight Distribution

| sample ^a | M_n | M_w | M_z | M_w/M_n | M_z/M_w |
|---------------------|---------|---------|---------|-----------|-----------|
| PSH-A | 64 380 | 67 330 | 70 100 | 1.040 | 1.037 |
| PSD-A | 68 340 | 72 640 | 77 090 | 1.058 | 1.061 |
| PSH-B | 110 410 | 114 380 | 118 310 | 1.036 | 1.034 |
| PSD-B | 102 300 | 110 910 | 118 040 | 1.084 | 1.064 |

^a PSH and PSD are acronyms for protonated and deuterated polystyrene, respectively. A designates polymers used in part A, and B refers to parts B-1 and B-2.

effectively, incompressible. This allows the intensity to be expressed simply as the sum of two terms, one for the scattering from a single chain, and one for the total scattering.¹⁰ For mixtures in which the degree of polymerization is the same for both protonated and deuterated species

$$I(q) = I_s(q) + I_t(q) \quad (1a)$$

$$I_s(q) = (a_H - a_D)^2 x(1-x) N_p n^2 S_s(q) \quad (1b)$$

$$I_t(q) = [a_D x + (1-x)a_H - a_s]^2 N_p n^2 S_t(q) \quad (1c)$$

a_D and a_H are the scattering lengths of deuterated (labeled) and protonated monomers, and a_s is the scattering length of that fraction of a solvent molecule equal to the volume of one monomer unit. N_p is the total number of polymer molecules. x is the mole fraction of monomers that are labeled. n is the ratio of molecular weight, M , to monomer weight, M_0 , of a polymer molecule. $S_s(q)$ is the single-chain structure factor normalized to unity at $q = 0$.

$$S_s(q) = 1/n^2 \langle \sum_{i,j} e^{i\mathbf{q} \cdot (\mathbf{r}_i - \mathbf{r}_j)} \rangle \quad (1d)$$

and $S_t(q)$ is the total scattering structure factor

$$S_t(q) = K \langle \sum_{M,N,i,j} e^{i\mathbf{q} \cdot (\mathbf{R}_M + \mathbf{r}_i)} e^{-i\mathbf{q} \cdot (\mathbf{R}_N + \mathbf{r}_j)} \rangle \quad (1e)$$

K is a normalization constant chosen such that $S_t(q) = S_s(q)$ at infinite dilution. The momentum transfer wave vector is $\mathbf{q} = \mathbf{k}_i - \mathbf{k}_f$, where \mathbf{k}_i and \mathbf{k}_f are the incident and scattered neutron vectors. The scattering is elastic and axially symmetric so that the scattered intensity is a function only of the scalar $q = (4\pi/\lambda) \sin \theta_s/2$. \mathbf{r}_i and \mathbf{r}_j are the vectors connecting the i th and j th monomers to the center of mass (COM) of a given polymer molecule, and \mathbf{R}_M and \mathbf{R}_N are the vector positions of the COM of the M th and N th polymer molecules.

Equations 1 are written for a system in which the labeled and unlabeled molecules have the same degree of polymerization. The correct equations take a different form when the H and D molecules are of unequal length. A matched condition was fulfilled for the first part of this study, but this was not quite true for the second part (Table I). Since the difference in measured quantities is small, we have at this stage chosen to ignore the mismatch.

In principle, $S_s(q)$ provides a complete description of the distribution of pairs of monomer units within a polymer molecule. In the lowest q region $S_s(q)$ is a simple function of the centroidal radius of gyration, R_g , and the latter can be obtained from $S_s(q)$ without reference to any molecular model. If the q range below $qR_g = 1.0$ is marginally reached experimentally, as is true of the present data, two alternatives are available. First, R_g can be obtained by fitting $S_s(q)$ to a scattering function derived from a molecular model. Second, the measured data can be extended into $q = 0$ by an extrapolation based on a molecular model.¹⁶ Both alternatives have been undertaken in this study by using a Debye model for $S_s(q)$; these are compared below. The first has the advantage of using a much wider region of the q -space data, but it has the disadvan-

tage that the result is dependent on a model that may not accurately represent the real molecule.

The total scattering factor $S_t(q)$ contains information on both inter- and intramolecular geometric arrangements, but this information is less obvious than that extracted from $S_s(q)$. A simple approximate model, originally proposed by Edwards,¹⁷ provides a calculation of $S_t(q)$ in terms of a single parameter, the screening length, ξ . The variation of ξ with concentration is a measure of the relative contributions of inter- and intramolecular distances to the pair distribution function. Edwards obtained

$$S_t(q) = A/(1 + q^2\xi^2) \quad (2)$$

ξ decreases with increasing concentration. Equation 2 is based on a pair correlation function of the Debye-Hückel type. To the extent that the correct correlation function differs in form from the Debye-Hückel model, ξ becomes q dependent if obtained by fitting experiments to eq 2.

Experimental Procedure and Data Reduction

Measurements were made at the 30-m SANS spectrometer at the Oak Ridge HFIR reactor.¹⁸ Data for the first part of this study were taken in November 1982; data for the second part were taken in May 1983 and in August 1983. In all cases the neutron wavelength was 4.75 Å and the scattering geometry was held fixed. Diameters of the source and sample apertures were 2.0 and 1.0 cm, respectively; source-to-sample and sample-to-detector flight paths were 7.5 and 6.98 m, respectively. A 4.0 cm diameter gadolinium beamstop was used to mask the direct beam. For our polymer samples we believe this geometry gave usable data in the q range from 0.007 to 0.070 Å⁻¹.

Several detector characteristics should be noted. First, all data must be corrected for the q dependence of the detector efficiency. This is based on scattering intensities from H₂O measured by the ORNL staff at a sample-to-detector distance of 1.5–2.5 m (for good statistics); this is monitored during the detector life. The transfer of these efficiency profiles to our geometry apparently creates no anomalies within our q range. Second, changes in detector overall sensitivity were significant between acquisition periods but negligible during any given acquisition period (~1 week). This creates only a change in "machine constant" for each series and is independent of q . Third, small shifts in the q assigned to the ADC channel for each detector spatial position occurred between our ORNL visits, due to changes in the detector electronics calibration. This required small corrections in the measured values of R_g and ξ . These were determined by comparison measurements of R_g for a standard ORNL aluminum sample with ~0.7 vol % voids.¹⁹ To allow direct comparison of the data this required multiplying our measured values of R_g and ξ , taken in November 1982 and in May and August 1983, by the factors 0.993, 1.040, and 0.981, respectively. These factors agree very well with changes in R_g observed from repeated measurements of our 100% concentration (solid wafer) polystyrene samples.

All polymer solutions were prepared in deuteriotoluene. Toluene-deuteriotoluene mixtures were used for background corrections. Polystyrene (PSH) and deuterated polystyrene (PSD) were prepared by anionic polymerization and purchased from Polymer Laboratories, Inc., of the U.K. The molecular weights and molecular weight distributions were determined by gel permeation chromatography and are given in Table I.²⁰ Toluene was obtained from Mallinckrodt and perdeuteriotoluene (99.6% deuterium) from Merck Sharpe and Dohme. Both solvents were used as received. Molar volumes of deuterated and protonated species are equal. The partial specific volume

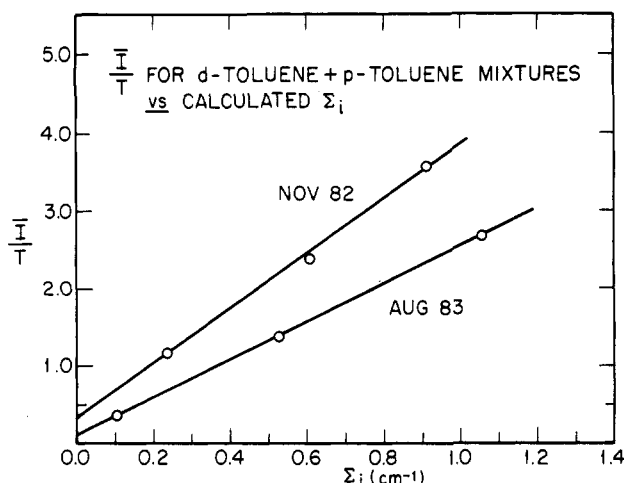


Figure 1. Transmission-corrected and q -averaged intensities from mixtures of toluene and deuteriotoluene as a function of the calculated macroscopic incoherent scattering cross section. The intensity renormalization between the two dates has been omitted to illustrate reproducibility.

of polystyrene in toluene has been widely studied.²¹ We have set this quantity equal to 0.92 in solution and 0.95 in bulk.

The solutions were contained in precision quartz cells. For all polymer concentrations $\leq 22\%$ mole fraction and for the solvent mixtures the solution thickness in the cells was fixed at 0.50 cm. Thinner cells were used for 35% and 50% concentrations for which the solution width was 0.20 cm. Bulk samples (100% polymer concentration) were hot pressed and slowly cooled under pressure through the glass transition. The solid wafers were approximately 0.10 cm thick.

These sample thicknesses were chosen to keep transmission factors greater than about 0.50. Measured transmission factors varied from 0.466 to 0.676 for $x = 0$ solution samples and from 0.630 to 0.766 for $x = 0.8$ solution samples. Empty quartz cells have a transmission of 0.957 ± 0.005 , so that the solution transmissions will be higher by a factor of 1.045.

To reach the coherent intensities of eq 1b and 1c the measured intensities must be normalized for sample thickness, transmission, and background. "Beam-blocked" (area) background and empty-cell scattering constitute very small corrections which are treated in the conventional manner. Removal of the larger incoherent background due to the sample solution itself is less obvious because of the presence of substantial fractions of coherent scattering solvent. We have made this correction by subtracting the measured scattering from a solvent mixture of toluene and deuteriotoluene for which the calculated macroscopic incoherent cross section Σ_i is equal to that calculated for the polymer solution in question. The solvent mixtures were contained in cells identical with the polymer solution cells and the count rates normalized and corrected exactly as for the sample intensities. Figure 1 gives measured intensities vs. calculated Σ_i for two series of solvent mixtures. Between q limits of 0.007 and 0.07 \AA^{-1} no systematic variation in intensity was observed, so that the average of the corrected intensity was used to improve statistics. Except for a relatively small nonzero intercept at $\Sigma_i = 0$ these curves are well fitted by an intensity law of the form

$$I = a \Sigma_i T_s = a \Sigma_i e^{-\Sigma_i t} \quad (3a)$$

where Σ_s and t are the solution total cross section and thickness. In our background correction treatment we have

used a "best fit" to the full curve

$$\bar{I}/T_s = a \Sigma_i + b \quad (3b)$$

The maximum corrections occur for solutions for which $x = 0$, but the effect on $I_s(q)$, eq 1b, is of primary interest. To illustrate the background magnitudes the ratio of background intensity to total intensity for the $x = 0.5$ and 0.8 polymer solutions at, say, $q = 0.02 \text{ \AA}^{-1}$ falls monotonically from about 8.5% for 2% concentrations to 1.0% for 50% and 100% concentrations.

Some observations on this background method are in order. The non zero intensity at $\Sigma_i = 0$ is probably real and, within composition and counting uncertainties, reproducible. This means a small but finite contribution to the solvent scattering must be attributed to coherent scattering. If the polymer solutions are incompressible, as has been assumed, all solvent coherent contributions have already been accounted for in eq 1c, and subtraction of this component is incorrect. However, because of the near equality of chemical composition between the toluene molecule and PSH monomer, the deuterated solvent fraction is perturbed very little when Σ_i is made the same for polymer and solvent mixtures. Inclusion of the small correction then seems justified. One may conjecture that it is present in the polymer scattering to nearly the same degree as in the solvent mixture and reveals a degree of compressibility. In any event, the contribution is apparently small and should constitute little error.

Finally, we have also explored carefully the alternative of finding the background by fitting the polymer scattering data to a Debye model plus an unknown background constant. In principle such a scheme improves the fit and this is what we have found. However, if the fitted equation is applied to data outside the q range used in fitting the function, errors are large and in some cases lead to negative intensities. We believe this is an unreliable procedure for obtaining the background corrections.

Experimental Results

$S_s(q)$ and $S_t(q)$ are obtained by subtraction of pairs of corrected intensities (eq 1a) from samples of the same polymer concentration but different x . Concentrations henceforth will be given in mole fraction of polymer, c , which we designate specifically by

$$c = n_M / (n_M + n_s) \quad (4)$$

where n_M and n_s are the number of moles of styrene monomer and of deuteriotoluene, respectively. The low molecular weight data of November 1982 will be identified as part A data. The sample names, x , and c identifications are given in Table II for part A data. Similarly the high molecular weight data of May 1983 will be named part B-1 and are given in Table III, while those of August 1983 are designated as part B-2 and given in Table IV.

For the data of part A, six solutions were measured for each of the two concentrations ($c = 8.0\%$ and 22%), corresponding to $x = 0.0, 0.20, 0.40, 0.60, 0.85$, and 1.00 . The $x = 1.00$ samples were not used because of poor intensities. $S_s(q)$ and $S_t(q)$ can be obtained from pairs of any of the remaining five samples. Figure 2 presents $S_s(q)$ and $S_t(q)$ for the 8% solutions. Three superposed curves are shown for $S_s(q)$, found from the pairs $x = 0.20$ and 0.40 , $x = 0.40$ and 0.60 , and $x = 0.60$ and 0.85 . $S_t(q)$ is obtained from the $x = 0.0$ sample. $S_t(q)$ for this case is relatively weak and flat. The ratio of $S_t(q)$ to $S_s(q)$ decreases with concentration. In Figure 2, and in all those to follow, the ordinates are, within a constant, equal to $S_s(q)$ and $S_t(q)$ multiplied by the polymer concentration, as obtained from the measured intensities of eq 1a-1c. The constant is fixed

Table II
Radii of Gyration and Intercepts from Part A Data

| sample description | | | | Zimm plot ^a | | Gaussian fit ^b | | |
|--------------------|------|------|-----------|------------------------|-------------------------------------|---------------------------|-------------------|-------------------|
| no. | c | x | pair name | $I(0)^{-1}$ | $\langle R_g \rangle_w, \text{\AA}$ | $I(0)$ | $R_g, \text{\AA}$ | intercept product |
| 1 | 0.08 | 0.00 | ST1 | | | | | |
| 3 | 0.08 | 0.20 | SS3A1 | 0.0255 | 81.3 | 39.4 | 82.0 | 1.005 |
| 5 | 0.08 | 0.40 | SS5A1 | 0.0266 | 79.9 | 38.3 | 82.2 | 1.019 |
| 7 | 0.08 | 0.60 | SS7A1 | 0.0267 | 80.2 | 38.2 | 82.7 | 1.020 |
| 9 | 0.08 | 0.85 | SS9A1 | 0.0266 | 81.5 | 38.1 | 83.5 | 1.013 |
| 2 | 0.22 | 0.00 | ST2 | | | | | |
| 4 | 0.22 | 0.20 | SS4A2 | 0.0274 | 75.2 | 37.2 | 78.1 | 1.019 |
| 6 | 0.22 | 0.40 | SS6A2 | 0.0281 | 73.6 | 36.3 | 76.9 | 1.020 |
| 8 | 0.22 | 0.60 | SS8A2 | 0.0262 | 75.4 | 38.6 | 77.4 | 1.011 |
| 10 | 0.22 | 0.85 | SS10A2 | 0.0273 | 76.0 | 37.1 | 78.1 | 1.013 |

^a $\tilde{q} = 0.00728$, $\hat{q} = 0.0208$. ^b $\tilde{q} = 0.00728$, $\hat{q} = 0.0409$.

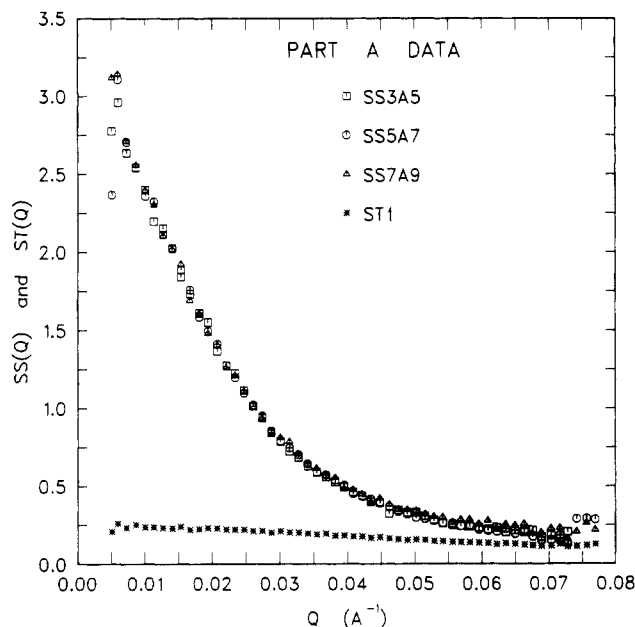


Figure 2. $S_s(q)$ and $S_t(q)$ for part A experiments, $c = 0.08$. $S_s(q)$ is obtained from three sample pairs, SS3A5, SS5A7 and SS7A9; $S_t(q)$ is obtained from sample ST1.

for a given molecular weight and spectrometer condition; no further normalization is made.

There is excellent reproducibility in the three plots of $S_s(q)$, and this remains so for all other combinations of x available. The same statement applies to determinations of $S_t(q)$, but reproducibility is limited by much poorer counting statistics and by the fact that it is the small difference of large numbers. For this reason $S_t(q)$ is most clearly defined by the $x = 0.0$ sample alone. Figure 3 shows three determinations of $S_t(q)$. Figure 4 gives the results of the same x pairings for the 22% samples. Again the superposition is excellent and extends to all available pairs.

The determination of $S_s(q)$ and $S_t(q)$ for the higher molecular weight data, parts B-1 and B-2, follows the procedure for part A, but with less redundancy. Solution concentrations for $c = 2.0\%$, 3% , 4% , 6% , 8% , 12% , 16% , 22% , 35% , 50% and solid samples for $c = 100\%$ were prepared. In each case three samples were made, corresponding to $x = 0.0$, 0.50 , and 0.80 . The first of these gives $S_t(q)$ directly. The coefficient of $S_t(q)$ is calculated to vanish at $x = 0.80$ and hence gives $S_s(q)$ only. $x = 0.50$ gives maximum scattering intensity and is used with $x = 0.0$ data to obtain a second measure of $S_s(q)$. The agreement of the two values of $S_s(q)$ is generally very good, but for some samples less satisfactory than in part A. Examples of good redundancy are shown for $c = 2.0\%$ in Figure 5 and for $c = 12.0\%$ in Figure 6. For a few samples, this

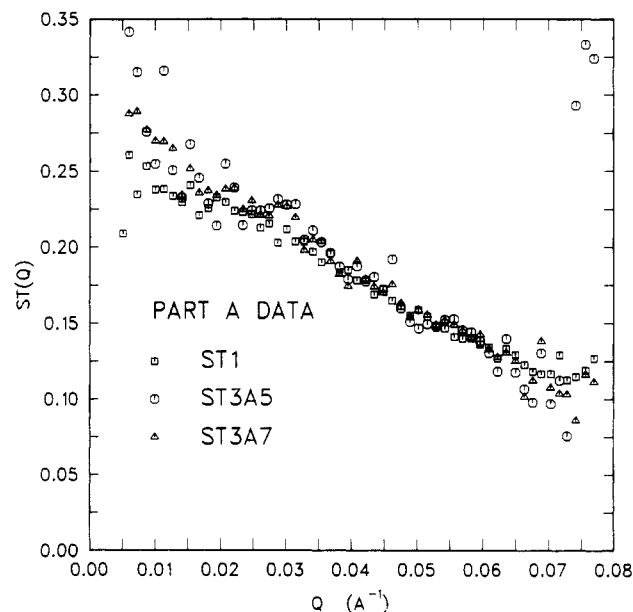


Figure 3. $S_t(q)$ determined from sample ST1, and from the two pairs 3 and 5, and 3 and 7.

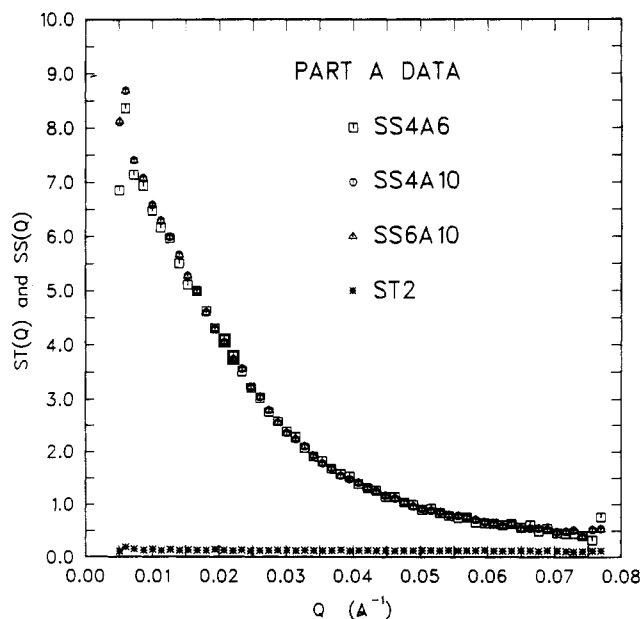


Figure 4. $S_s(q)$ and $S_t(q)$ for part A experiments, $c = 0.22$. $S_s(q)$ is obtained from three sample pairs SS4A6, SS4A10, and SS6A10; $S_t(q)$ is from sample ST2.

comparison was poor enough to eliminate the use of the data. Specifically the B-1 data for $c = 2.0\%$ ($x = 0.5$ and $x = 0.8$) and the B-2 data for $c = 50.0\%$ ($x = 0.5$) were not

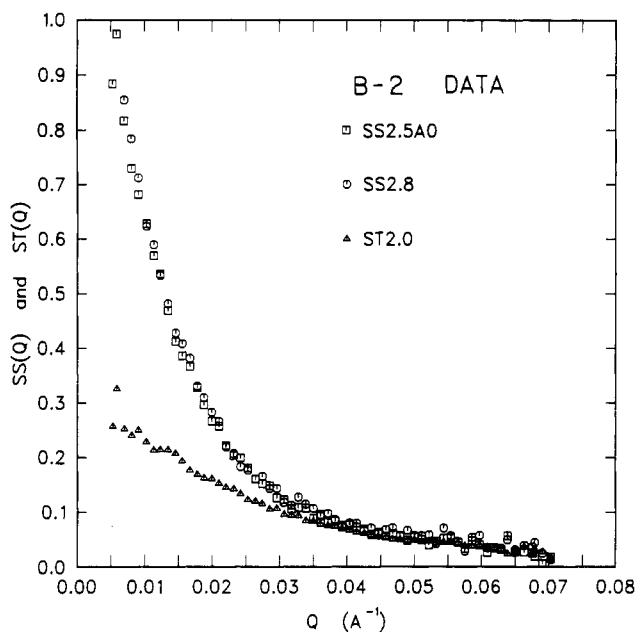


Figure 5. Scattering functions from part B-2 data for $c = 0.02$. Two measurements of $S_s(q)$ are shown, for SS2.8 and for the pair SS2.5A0.

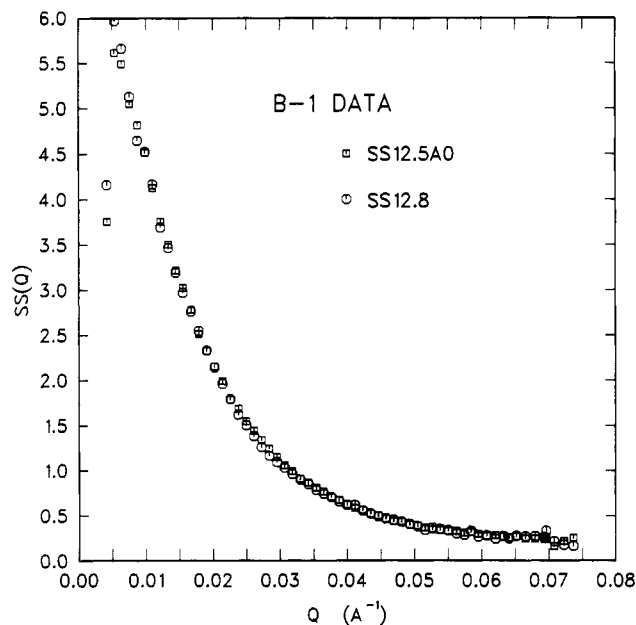


Figure 6. $S_s(q)$ measured from part B-1 data.

used. Figure 7 illustrates the disagreement observed for the 2.0% (B-1) data.

Figure 8 is a plot of the ratio $S_s(q)/S_t(q)$ for c varying from 2% to 16%, at a q value of 0.0145 \AA^{-1} . Within experimental error the ratio converges to unity as c goes to zero. This convergence is also observed at lower and higher values of q .

Determination of R_g and ξ

As stated above, R_g has been obtained by two methods. In one we follow the suggestion, first made by Zimm,²² of plotting c/I vs. q^2 . For this work we find the curve of $S_s(q)^{-1}$ vs. q^2 and call it a Zimm plot. Our measurements extend down to $q = 0.007 \text{ \AA}^{-1}$ only, and we find enough curvature in this q region to require theoretical extrapolations to lower q . This correction is based on a Gaussian coil model and includes the effect of polydispersity.¹⁶ The corrections to the measured intercepts at $q = 0$ are of order

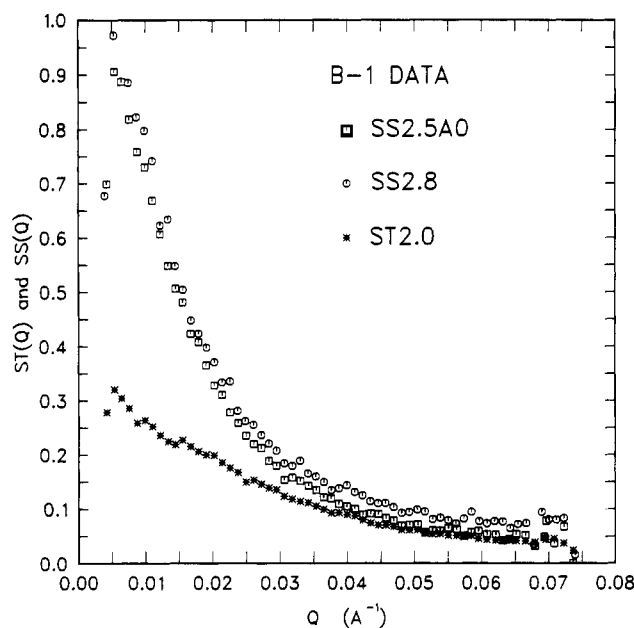


Figure 7. Scattering functions from part B-1 data, $c = 0.02$, showing poor coincidence for SS2.8 and SS2.5A0. These results were discarded.

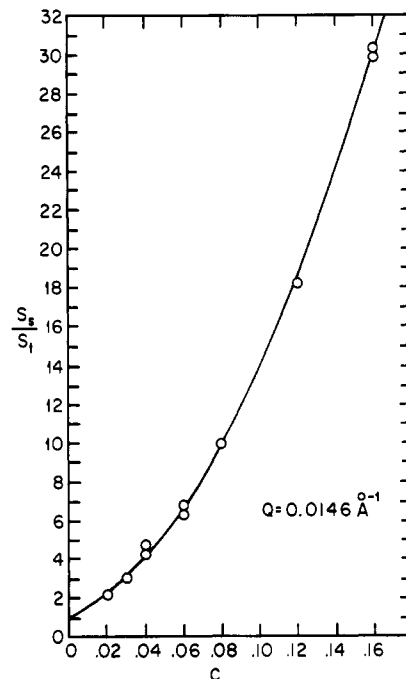


Figure 8. Ratio of the normalized scattering functions $S_s(q)/S_t(q)$ plotted for $q = 0.0146 \text{ \AA}^{-1}$ as a function of c .

5–10%. The corrections to the values of R_g are of order 5–15%. The range of measured points used in the Zimm plots extended from 0.07 to 0.02 \AA . The upper limit was chosen to give an adequate number of experimental points and at the same time restrict the magnitude of qR_g . The choice was made after several numerical experiments, but the corrected values of R_g were only slightly sensitive to this choice.

The experimental $S_s(q)$ curves were also fitted to a Gaussian coil model. The scattering from such a coil was found by Debye²³ to be

$$F_D(x) = (2/x^2)(x - 1 + e^{-x}) \quad (5a)$$

where

$$x = q^2 R_g^2 \quad (5b)$$

Table III
Radii of Gyration and Intercepts from Part B-1 Data

| sample description | | | Zimm plot ^a | | Gaussian fit ^b | | intercept product |
|--------------------|----------|-----------|------------------------|-------------------------------------|---------------------------|-------------------|-------------------|
| <i>c</i> | <i>x</i> | pair name | $I(0)^{-1}$ | $\langle R_g \rangle_w, \text{\AA}$ | $I(0)$ | $R_g, \text{\AA}$ | |
| 0.04 | 0.0 | ST4.0 | | | | | |
| 0.04 | 0.5 | SS4.5A0 | 0.02062 | 113.1 | 51.66 | 119.3 | 1.065 |
| 0.04 | 0.8 | SS4.8 | 0.01937 | 114.6 | 52.56 | 119.4 | 1.018 |
| 0.06 | 0.0 | ST6.0 | | | | | |
| 0.06 | 0.5 | SS6.5A0 | 0.01993 | 111.0 | 51.51 | 116.0 | 1.027 |
| 0.06 | 0.8 | SS6.8 | 0.01888 | 113.0 | 54.50 | 118.8 | 1.029 |
| 0.08 | 0.0 | ST8.0 | | | | | |
| 0.08 | 0.5 | SS8.5A0 | 0.01960 | 109.9 | 51.99 | 113.4 | 1.019 |
| 0.12 | 0.0 | ST12.0 | | | | | |
| 0.12 | 0.5 | SS12.5A0 | 0.01933 | 107.1 | 52.37 | 109.8 | 1.012 |
| 0.12 | 0.8 | SS12.8 | 0.01955 | 106.3 | 52.61 | 111.4 | 1.028 |
| 0.16 | 0.0 | ST16.0 | | | | | |
| 0.16 | 0.5 | SS16.5A0 | 0.01992 | 104.1 | 51.42 | 108.7 | 1.024 |
| 0.16 | 0.8 | SS16.8 | 0.01932 | 104.8 | 53.44 | 110.4 | 1.032 |
| 0.22 | 0.0 | ST22.0 | | | | | |
| 0.22 | 0.5 | SS22.5A0 | 0.01999 | 101.6 | 50.90 | 105.4 | 1.017 |
| 0.22 | 0.8 | SS22.8 | 0.01820 | 105.9 | 55.93 | 109.6 | 1.018 |
| 0.35 | 0.0 | ST35.0 | | | | | |
| 0.35 | 0.5 | SS35.5A0 | 0.01990 | 97.5 | 52.16 | 99.7 | 1.038 |
| 0.35 | 0.8 | SS35.8 | 0.01801 | 98.5 | 56.14 | 101.4 | 1.011 |
| 0.50 | 0.0 | ST50.0 | | | | | |
| 0.50 | 0.5 | SS50.5A0 | 0.02111 | 91.8 | 48.62 | 96.7 | 1.026 |
| 0.50 | 0.8 | SS50.8 | 0.01701 | 96.2 | 59.79 | 99.6 | 1.017 |
| 1.00 | 0.0 | ST100.0 | | | | | |
| 1.00 | 0.5 | SS100.5A0 | 0.01729 | 89.9 | 58.57 | 92.9 | 1.013 |
| 1.00 | 0.8 | SS100.8 | 0.01576 | 96.0 | 63.57 | 97.0 | 1.002 |

^a $\bar{q} = 0.00757$, $\hat{q} = 0.0203$. ^b $\bar{q} = 0.00757$, $\hat{q} = 0.0411$.

Table IV
Radii of Gyration and Intercepts from Part B-2 Data

| sample description | | | Zimm plot ^a | | Gaussian fit ^b | | intercept product |
|--------------------|----------|-----------|------------------------|-------------------------------------|---------------------------|-------------------|-------------------|
| <i>c</i> | <i>x</i> | pair name | $I(0)^{-1}$ | $\langle R_g \rangle_w, \text{\AA}$ | $I(0)$ | $R_g, \text{\AA}$ | |
| 0.02 | 0.0 | ST2.0 | | | | | |
| 0.02 | 0.5 | SS2.5A0 | 0.01926 | 122.9 | 52.52 | 125.6 | 1.012 |
| 0.02 | 0.8 | SS2.8 | 0.01872 | 120.4 | 54.32 | 123.4 | 1.017 |
| 0.03 | 0.0 | ST3.0 | | | | | |
| 0.03 | 0.5 | SS3.5A0 | 0.02014 | 120.6 | 49.84 | 122.8 | 1.004 |
| 0.03 | 0.8 | SS3.8 | 0.01960 | 123.0 | 51.24 | 124.9 | 1.004 |
| 0.04 | 0.0 | ST4.0 | | | | | |
| 0.04 | 0.5 | SS4.5A0 | 0.02029 | 116.4 | 49.62 | 118.7 | 1.007 |
| 0.04 | 0.8 | SS4.8 | 0.01873 | 121.0 | 53.42 | 122.2 | 1.001 |
| 0.06 | 0.0 | ST6.0 | | | | | |
| 0.06 | 0.5 | SS6.5A0 | 0.02054 | 115.1 | 48.73 | 116.6 | 1.001 |
| 0.06 | 0.8 | SS6.8 | 0.01993 | 116.4 | 49.97 | 117.1 | 0.995 |
| 0.16 | 0.0 | ST16.0 | | | | | |
| 0.16 | 0.5 | SS16.5A0 | 0.02079 | 105.2 | 48.33 | 107.3 | 1.005 |
| 0.16 | 0.8 | SS16.8 | 0.02043 | 104.4 | 49.83 | 108.2 | 1.018 |
| 0.22 | 0.0 | ST22.0 | | | | | |
| 0.22 | 0.5 | SS22.5A0 | 0.02120 | 100.4 | 47.64 | 103.4 | 1.010 |
| 0.22 | 0.8 | SS22.8 | 0.01955 | 103.2 | 50.88 | 105.8 | 0.995 |
| 0.35 | 0.0 | ST35.0 | | | | | |
| 0.35 | 0.5 | SS35.5A0 | 0.02031 | 99.8 | 49.13 | 100.8 | 0.998 |
| 0.35 | 0.8 | SS35.8 | 0.01942 | 99.5 | 51.57 | 102.3 | 1.001 |
| 0.50 | 0.0 | ST50.0 | | | | | |
| 0.50 | 0.5 | SS50.5A0 | 0.0218 | 94.2 | 44.55 | 91.5 | 0.971 |
| 0.50 | 0.8 | SS50.8 | 0.02144 | 95.5 | 47.22 | 98.6 | 1.012 |
| 1.00 | 0.0 | ST100.0 | | | | | |
| 1.00 | 0.5 | SS100.5A0 | 0.01940 | 88.2 | 52.17 | 91.4 | 1.012 |
| 1.00 | 0.8 | SS100.8 | 0.01744 | 95.8 | 57.06 | 96.0 | 0.995 |

^a $\bar{q} = 0.00700$, $\hat{q} = 0.01995$. ^b $\bar{q} = 0.00700$, $\hat{q} = 0.0404$.

A curve-fitting program²⁴ was used to minimize the function $[S_s(q) - AF_D(qR_g)]^2$, where R_g and the intercept A are unknown parameters. In principle, eq 5a is the correct description for a flexible chain in bulk in a θ solvent. In a good solvent, excluded volume effects enter and neither the scattering function nor the chain statistics are known. However, recent theoretical work by Witten and Schaefer²⁵ and also by Ohta, Oono, and Freed²⁶ show that the scattering intensity of a very high molecular weight

chain in a good solvent is close to that of a Gaussian coil. This gives some support to our use of the Debye result.

We have also performed some numerical experiments with the Ptitsyn model of a polymer in a good solvent. In this model, the mean square distance between the monomer units i and j is proportional to $|i - j|^{2\nu}$, where ν is greater than 0.5, and the distribution function is taken to be Gaussian. Our procedure was to fit the experimental $S(q)$ to the scattering function calculated by Ptitsyn.²⁷ If

Table V
Parameters for Power Law $R_g^2 = Kc^{-n}$

| expt | fitting method | x | constant K | exponent n |
|-----------|----------------|-----------|----------------|-------------------|
| B-1 | Gaussian | 0.5 | 8550 \pm 100 | 0.162 \pm 0.006 |
| B-2 | Gaussian | 0.5 | 8420 \pm 100 | 0.165 \pm 0.002 |
| B-1 | Zimm | 0.5 | 8000 \pm 160 | 0.156 \pm 0.010 |
| B-2 | Zimm | 0.5 | 7960 \pm 250 | 0.173 \pm 0.012 |
| B-1 | Gaussian | 0.8 | 9240 \pm 210 | 0.143 \pm 0.012 |
| B-2 | Gaussian | 0.8 | 8880 \pm 250 | 0.158 \pm 0.012 |
| B-1 | Zimm | 0.8 | 8850 \pm 230 | 0.125 \pm 0.013 |
| B-2 | Zimm | 0.8 | 8510 \pm 240 | 0.160 \pm 0.013 |
| B-1 + B-2 | Gaussian | 0.5 + 0.8 | 8770 \pm 90 | 0.157 \pm 0.005 |
| B-1 + B-2 | Zimm | 0.5 + 0.8 | 8330 \pm 130 | 0.154 \pm 0.007 |

the Ptitsyn function is written $F_p(qR_g, \nu)$ the curve fitting minimized $[S_i(q) - AF_p(qR_g, \nu)]^2$ where now A , R_g , and ν are allowed to vary. The result led to $\nu = 0.5$ as the best exponent. Again this result tends to support use of the Debye model.

The upper and lower limits of q selected for fitting the Debye curves were 0.007 and 0.040 \AA^{-1} . As found by trials with other high q limits, this choice covers the important range of intensity changes without suffering minor data anomalies at higher q . However, the fitted parameters are not significantly changed by extending the limit to 0.07 \AA^{-1} .

Both the extrapolated Zimm plots and Gaussian least-squares-fitted curves were used to generate values of R_g and scattering intensities at $q = 0$. The Zimm plots give a z -average radius of gyration. These were corrected to weight averages by multiplying by an average $(M_w/M_z)^{1/2}$. If polydispersity is included in the Gaussian coil fitting, the Debye formula is modified.²⁸ The differences in R_g between using eq 5a and the modified formula were calculated and averaged 0.3%, with a maximum of 0.7% in one case. The corrections are small and were ignored.

Screening lengths were obtained by using Zimm plots of the $S_i(q)$ data points (for $x = 0.0$). Because the $S_i(q)$ profiles are relatively flat and weak, it was undesirable to use the data extending to lowest q . The fitting interval selected ranged from approximately 0.017 to 0.052 \AA^{-1} . We found the numerical values became quite erratic at high concentration, and we have reported results only for $c \leq 0.22$.

The numerical values of R_g and intercept, determined by both fits, are shown in Table II for the scattering data of part A. For both concentrations $x = 0.0$ was used paired with the remaining x values to give four redundant measurements. The R_g 's and intercepts, again using both methods of fitting, are given in Table III for the measurements of part B-1, and in Table IV for those of part B-2. The B-1 and B-2 data have been kept separate to reveal any cumulative effect of several small differences between the two experimental runs. Results from $x = 0.5$ (with $x = 0.0$) and $x = 0.8$ should be redundant. The numerical intercepts are those obtained from fitting the functions such as are displayed in Figures 2-6, but divided by the polymer concentrations. Since for the two fitting methods these should be reciprocals, their product should be unity. A column giving these products is included in the tables. Table V gives the values of R_g from the fitting of B-1 and B-2 data.

Critique of Experimental Results

The figures in Table II for the lower molecular weight measurements of part A show the same internal consistency as shown by the scattering functions of Figure 2-4. The reproducibility in R_g and in the intercepts, for the Gaussian fitting method, is of order 1% for both the 0.08

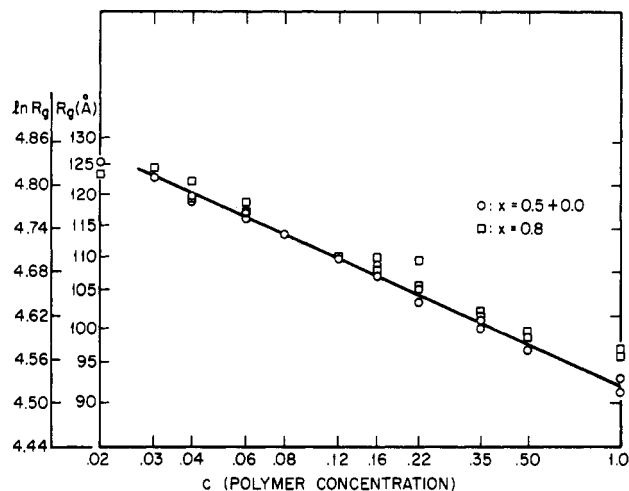


Figure 9. Logarithmic plot of R_g vs. c for R_g determined by fitting scattering functions of B-1 and B-2 experiments to a Gaussian model. The open circles are from sample pairs with $x = 0.50$ and $x = 0.0$; the squares are from samples with $x = 0.80$. The straight line is a least-squares fit to the sample pairs for $x = 0.50$ and $x = 0.0$, from $c = 0.03$ to $c = 1.0$.

and 0.22 concentrations. Other sample pair selections show agreement at least this good. The reproducibility is also of order 1% for the Zimm plot fitting of the 0.22 data but is nearer 2% for the 0.8 data due to one low point. The Gaussian fits lead to $R_g(0.08) = 82.6 \pm 0.8 \text{ \AA}$ and $R_g(0.22) = 77.6 \pm 0.7 \text{ \AA}$. The values from Zimm fitting are 80.7 ± 0.8 and $75.1 \pm 1.5 \text{ \AA}$. The ratios $R_g(0.08)/R_g(0.22)$ for the two methods are equal within statistics, but the Zimm fits of both R_g 's are systematically lower than the Gaussian fits by 2-3%. There is no question that R_g is falling as c increases. We are left with the conclusion that while the magnitudes of R_g are somewhat altered by the fitting scheme, the variation of R_g with concentration is not.

The internal consistency in the parameters for the higher molecular weight solutions given in Tables III and IV is reasonable but somewhat poorer than for the lower weight results. The sample solutions were remade between runs B-1 and B-2, yet the values of R_g for the same concentration and x compare well between the two runs. There is, however, a persistent difference, evident in both sets, for R_g measured from samples made with $x = 0.5$ as opposed to those for which $x = 0.8$. The numbers for $x = 0.8$ are higher than those for $x = 0.5$; the average ratio is 1.02. We suspect this systematic difference is due to the mismatch in the degree of polymerization for the PSH-B and PSD-B polymer materials. The correction has been ignored but will be addressed. The solid wafers for $c = 1.0$ were not remade between runs B-1 and B-2. For a given x the reproducibility between runs is good, as expected, but the largest discrepancy between $x = 0.5$ and $x = 0.8$ data occurs for these solid samples. Here, however, we cannot rule out the existence of forward scattering due to the presence of voids, which may be different between wafers. It is significant, in this context, that the R_g 's from samples for which $x = 0.5$ are in very good agreement with the several published^{14,15} values for polystyrene either in a θ solvent or in bulk, whereas those for samples with $x = 0.8$ are considerably higher (and, incidentally, the R_g for the same bulk sample of Daoud et al.⁴ is considerably lower).

The R_g 's determined by Gaussian fit in Tables III and IV are exhibited in the logarithmic plot of Figure 9 (we have assumed SS50.5A0 shows anomalous error and henceforth omit it). It is evident that the points for $x = 0.5$ lying above $c = 0.02$ are well fitted by a straight line

Table VI
Screening Lengths from Data of Parts B-1 and B-2^a

| <i>c</i> | ξ , Å | |
|----------|-----------|-------|
| | (B-1) | (B-2) |
| 0.02 | 44.2 | 44.3 |
| 0.03 | | 34.3 |
| 0.04 | 24.4 | 28.5 |
| 0.06 | 21.8 | 20.0 |
| 0.08 | 17.1 | |
| 0.12 | 13.3 | |
| 0.16 | 9.4 | 9.9 |
| 0.22 | 9.0 | 8.3 |

^a $x = 0.0$, $\tilde{q} = 0.017 \text{ Å}^{-1}$, $\tilde{q} = 0.052 \text{ Å}^{-1}$.

with little scatter. The points for $x = 0.8$ show greater scatter and lie above the $x = 0.5$ data by an average factor of 1.02.

All of the radii given in Tables III and IV, above $c = 0.02$, have been fitted, by linear regression, to a power law of the form $R_g^2 = Kc^{-n}$. To reveal the sensitivity of the parameters to the choice of x , to the fitting method, and to the experimental run, the parameters have been determined separately for each condition. These are listed in Table V together with the deviations from the mean. The solid curve shown in Figure 9 is fitted to the sum of R_g ($x = 0.5$) Gaussian points from both B-1 and B-2 experiments. Included also in Table V are power-law parameters using all the R_g 's (again above $c = 0.02$) determined by Gaussian fitting, and again when determined by Zimm plots.

We are tempted, for the several reasons noted above, to select as most reliable the parameters determined by Gaussian fitting and restricted to $x = 0.5$ samples. This gives $K = 8480 \pm 100 \text{ Å}^2$, $n = 0.163 \pm 0.006$. However, we have elected instead to include all the data and average over fitting methods. This leads us to the parameters $K = 8550 \pm 130 \text{ Å}^2$, $n = 0.156 \pm 0.012$. The two choices are well within the error limits.

The determination of ξ from $S_i(q)$ is based on measurements with poorer statistics, and these become unacceptable for data above $c = 0.22$. Table VI gives the magnitudes of ξ obtained from the Zimm plots of all B-1 and B-2 samples for which $x = 0.0$. These points have been fitted to a power law of the form $\xi = K_1 c^{-m}$ and are displayed in Figure 10. A surprisingly good profile is obtained for $K_1 = 2.89 \pm 0.15 \text{ Å}$ and $m = 0.70 \pm 0.02$.

Interpretation of Experiments

The prevalent renormalization and scaling theories for predicting the variation of R_g and ξ with concentration are based on viewing the polymer molecule as a physical system near its critical point. According to the formalism, we may write

$$R_g^2 = Kc^{(1-2\nu)/(3\nu-1)} \quad (6a)$$

$$\xi = K_1 c^{-\nu/(3\nu-1)} \quad (6b)$$

where ν and R_g are related by $R_g \sim M^\nu$ for a highly dilute solution. In a Θ solvent, $\nu = 0.5$, and in a good solvent $\nu = 0.6$ according to a "mean field" theory.^{29,30} According to an analysis of the renormalization group type, $\nu = 0.588$.³¹ These lead to the exponents $R_g^2 \sim c^{0.0}$, $c^{-0.25}$, and $c^{-0.23}$ and $\xi \sim c^{-1.0}$, $c^{-0.75}$, and $c^{-0.77}$, respectively.

In fact, it is well-known that ν is an increasing function of molecular weight. A precise measurement, by Einaga et al.,³² of the intrinsic viscosity of polystyrene in benzene and in cyclohexane leads us to believe that $\nu \approx 0.57$ may be a "best" choice for our molecular weight range. We assume benzene is an acceptable surrogate for toluene.

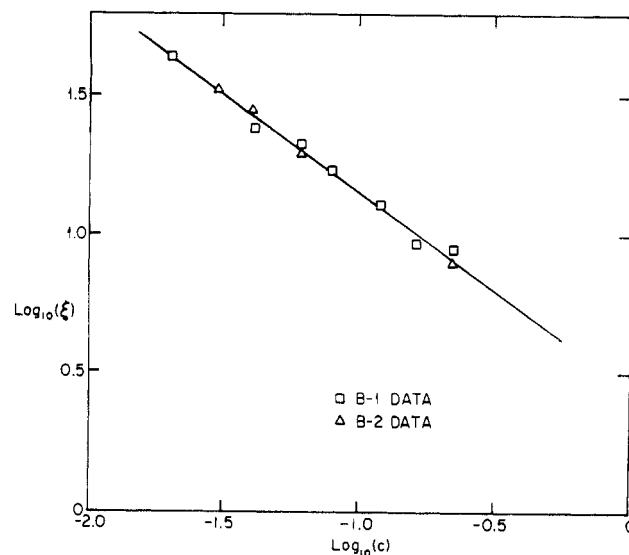


Figure 10. Logarithmic plot of screening length ξ . Concentrations from $c = 0.02$ to 0.22 only are used in the power-law fit.

There is some reason to believe³³⁻³⁵ that the exponent derived from viscosity is slightly lower than that which applies to R_g and ξ , but this difference has little effect here. For $\nu = 0.57$ the scaling laws yield $R_g^2 \sim c^{-0.20}$ and $\xi \sim c^{-0.80}$.

The scaling laws are designed for semidilute solutions, and it is impossible to determine a specific lower limit for c . The choice depends on c^* , a concentration which marks the end of the dilute regime. One recipe⁴ for c^* is based on the equation $N_p(R_g)^3 = 1$, where N_p is the number of polymers per unit volume. Another estimate³⁶ is based on $c^* = 0.77[\eta]$, where $[\eta]$ is the intrinsic viscosity. For the polymers used in our B-1, B-2 measurements these lead to $c^* \approx 0.11 \text{ g/mL}$ and $c^* \approx 0.014 \text{ g/mL}$. Other suggestions fall between these wide limits. This leaves the experimentalist with a broad latitude in fitting the semidilute limit. We find our data can be well fitted to a power law for all c from 0.03 to 1.0 , but not from 0.02 to 1.0 . The leveling off is evident in Figure 9; inclusion of the 0.02 points would lower the magnitude of the concentration exponent. For our purpose c^* is that concentration above which $\ln R_g$ is linear in $\ln c$.

The SANS measurements reported by Daoud et al.⁴ were applied to polystyrene of $M_w = 114000$, dissolved in CS_2 , for polymer concentrations from $c = 0.03 \text{ (g/mL)}$ to $c = 1.06 \text{ (bulk state)}$. The concentration coefficient was assigned the value 0.25 ± 0.02 . From their tabulated data for all of these concentrations, we find their result to be $R_g^2 = 7013c^{-0.225}$, while removal of the $c = 0.03$ point (which falls off their power-law fit) gives $6822c^{-0.250}$. We find their bulk value for R_g lies well below the values established in other experiments.^{3,14,15} If both points $c = 0.03$ and $c = 1.05$ are removed, the fit becomes $R_g^2 = 7265c^{-0.210}$. All of these coefficients lie outside the error limits assigned to our experiments, and we must conclude that there is a definite disagreement between the two.

The measured dependence of the screening length on concentration differs somewhat from that predicted by scaling theory; our value for the coefficient $m = 0.70 \pm 0.02$ is to be compared to 0.75 , applicable to a very large polymer chain, and to 0.80 , which results from our estimate for the lower molecular weight used in this experiment. There are several measurements of ξ reported for polystyrene in benzene. Cotton et al.³⁷ measured samples of molecular weight 6.5×10^5 and 2.1×10^6 , and we find the best fits to those data, from logarithmic plots, are $\xi = 2.97c^{-0.72}$ and $2.96c^{-0.74}$. A similar fit to the data presented

Table VII
Calculated Excluded Volume Parameter vs. c

| c | w | |
|------|----------|----------|
| | B-1 data | B-2 data |
| 0.02 | 1.211 | 1.466 |
| 0.03 | | 1.559 |
| 0.04 | 2.052 | 1.575 |
| 0.06 | 1.626 | 1.739 |
| 0.08 | 1.799 | |
| 0.12 | 2.015 | |
| 0.16 | 2.997 | 2.629 |
| 0.22 | 2.137 | 2.463 |

by Daoud et al.⁴ (samples A–D of their Table III) leads us to a $\xi = 2.29c^{-0.79}$. Earlier light scattering measurements for a M_w of 7.5×10^6 by Benoit and Picot³⁸ yield $6.51c^{-0.67}$. The amplitude and limiting slope of ξ vs. c for several higher M_w polystyrene-toluene solutions have been reported by Wiltzius et al.³⁹ The slope is in exact agreement with our results and the amplitudes also agree well. It is thus apparent that our concentration dependence is, within experimental error, in agreement with values reported for considerably higher molecular weights. There may be a q dependence in ξ not revealed in our determination. Our lower q limit was chosen simply to avoid some low- q anomalies in the data.

An analysis of the dependence of screening lengths and molecular dimensions on concentration has been presented by Muthukumar and Edwards (ME).⁷ Their results have two striking advantages over that given in earlier scaling and renormalization calculations. First, the general equations apply at all concentrations, not only in a restricted range. Second, these are equations and not simply proportionalities, and consequently comparison between experiment and theory provides a stricter test of the theoretical agreement. Their general results are

$$\xi^{-2} = 6w\rho l / [l_1(1 + 27w\xi/8\pi l_1^2)] \quad (\text{ME-1.3a})$$

$$l_1^3(1/l - 1/l_1) = \alpha w\xi \quad (\text{ME-1.3b})$$

If L is the chain length, the mean square end-to-end lengths are $\langle R_w^2(\theta) \rangle = Ll$ under θ conditions and $\langle R_w^2 \rangle = Ll_1$ in general. The end-to-end distances are simply related to the measured radii of gyration by $R_w^2 = 6R_g^2/\delta$, where δ is a constant close to unity; we calculate it to lie between 0.98 and 1.0 from the estimates of Domb and Barrett.⁴⁰ ρ is the monomer concentration. w is the excluded volume parameter, which can be calculated from eq ME-1.3a from measured values of ξ and R_g . In principle w should be a constant independent of c . In Table VII we list calculated values of w for c varying from 0.02 to 0.22. An approximate average value of \bar{w} can be obtained; using concentrations from $c = 0.03$ to 0.12 only, we find $\bar{w} = 1.77 \pm 0.20 \text{ \AA}$.

Summary

It has been demonstrated that the high-concentration technique¹⁰ can be applied to obtain $S_s(q)$ for polymer solutions with a precision that exceeds all other experimental errors in a SANS measurement. The degree of polymerization should be closely matched between protonated and deuterated species. The method has been used to obtain the change in the R_g of polystyrene for concentrations ranging from 2% to bulk polymer. We find the power law $R_g^2 \sim c^{-0.156 \pm 0.012}$ fits the data from $c = 0.03$ to $c = 1.0$. This concentration exponent is substantially below that predicted from scaling theory as well as below the experimental exponent reported by Daoud et al.⁴ for the same polymer molecule dissolved in CS_2 . While the q range used by us required some analytic modeling or extrapolation, we do not believe this has jeopardized the

measured concentration dependence. We conclude that the difference between our result and that predicted by scaling theory demonstrates the inapplicability of the theory to the low- M_w polymer used here. This is apparently consistent with other tests of the theory.⁴¹ We have examined the experimental limits and reproducibility with particular care and, within these limits, we find that the concentration dependence shows no evidence of change from the lower limit of the semidilute region to the bulk polymer.

Measurements of the screening length as a function of concentration were also made. Reliable data were obtained in the restricted range $c = 0.02$ – 0.22 , and in the q range above 0.015 \AA^{-1} due to experimental limitations. The data fit a concentration dependence in agreement, within experimental limits, with published results both for M_w comparable to this work⁴ and for much higher M_w .^{37,38} Our measurement is closer to that predicted by asymptotic scaling theory than to that assumed by us to better represent the lower M_w regime used here. It does not appear possible to find a value of ν that simultaneously satisfies both eqs 6 for our measured values of R_g and ξ .

Acknowledgment. We thank A. Z. Akcasu, G. C. Summerfield, and C. C. Han for their observations during this study. P. Goyal made useful measurements leading into this work. W. C. Koehler and H. R. Child freely gave their guidance on spectrometer details. This work was supported by National Science Foundation Grant No. DMR-8217460.

Registry No. Polystyrene (homopolymer), 9003-53-6; neutron, 12586-31-1.

References and Notes

- (1) The random-flight model of a polymer chain in bulk polymer is implicit in the work of: Kuhn, W. *Kolloid.-Z.* 1934, 2, 68.
- (2) The concept of complete screening of excluded volume interactions in 100% polymer is most clearly enunciated in: Flory, P. J. "Principles of Polymer Chemistry"; Cornell University Press: Ithaca, NY, 1953; Chapter 14.
- (3) The experimental verification of the random-flight model has been verified by small-angle neutron scattering in a number of instances. See, for example: Benoit, H.; Cotton, J. P.; Decker, D.; Farnoux, B.; Higgins, J.; Jannink, G.; Ober, R.; Picot, C.; des Cloizeaux, J. *Macromolecules* 1974, 6, 863. Wignall, G. D.; Ballard, D. G. H.; Schelten, J. *Eur. Polym. J.* 1974, 15, 682. Kirste, R. G.; Kruse, W. A.; Ibel, K. *Polymer* 1975, 16, 120.
- (4) Daoud, M.; Cotton, J. P.; Farnoux, B.; Jannink, G.; Sarma, G.; Benoit, H.; Duplessix, R.; Picot, C.; de Gennes, P. G. *Macromolecules* 1975, 8, 804.
- (5) des Cloizeaux, J. *J. Phys. (Paris)* 1975, 36, 281.
- (6) de Gennes, P. G. "Scaling Concepts in Polymer Physics"; Cornell University Press: Ithaca, NY, 1979; Chapter 3.
- (7) Muthukumar, M.; Edwards, S. F. *J. Chem. Phys.* 1982, 76, 2720.
- (8) Some information on this question appears in a series of papers by Richards et al. Corrections for intermolecular interactions are not made in all cases, and it is difficult to extract a reliable measure of concentration variation of molecular size from that work. Richards, R. W.; Maconnachie, A.; Allen, G. *Polymer* 1978, 19, 266; *Polymer* 1981, 22, 147, 153, 158.
- (9) Williams, C. E.; Nierlich, M.; Cotton, J. P.; Jannink, G.; Boue, F.; Daoud, M.; Farnoux, B.; Picot, C.; de Gennes, P. G.; Riando, M.; Moan, M.; Wolf, C. *J. Polym. Sci., Polym. Lett. Ed.* 1979, 17, 379.
- (10) Akcasu, A. Z.; Summerfield, G. C.; Jahshan, S. N.; Han, C. C.; Kim, C. Y.; Yu, H. *J. Polym. Sci., Polym. Phys. Ed.* 1980, 18, 863.
- (11) Jahshan, S. N.; Summerfield, G. C. *J. Polym. Sci., Polym. Phys. Ed.* 1980, 18, 1859, 2419.
- (12) Summerfield, G. C. *J. Polym. Sci., Polym. Phys. Ed.* 1981, 19, 1011.
- (13) Benoit, H.; Koberstein, J.; Leibler, L. *Makromol. Chem., Suppl.*, 1981, 4, 85.
- (14) Tangari, C.; Summerfield, G. C.; King, J. S.; Berliner, R.; Mildner, D. F. *Macromolecules* 1980, 13, 1546. Tangari, C.; King, J. S.; Summerfield, G. C. *Macromolecules* 1982, 15, 132.

- (15) Wignall, G. D.; Hendricks, R. W.; Koehler, W. C.; Lin, J. S.; Wai, M. P.; Thomas, E. L.; Stein, R. S. *Polymer* 1981, 22, 886.
- (16) Recipes for the correction are given in: Ullman, R. *J. Polym. Sci., Polym. Lett. Ed.* 1983, 21, 521. Also: Ullman, R., submitted to *J. Polym. Sci., Polym. Lett. Ed.*
- (17) Edwards, S. F. *Proc. Phys. Soc.* 1966, 88, 265.
- (18) Koehler, W. C.; Hendricks, R. *J. Appl. Phys.* 1979, 50, 1951.
- (19) Child, H. R.; Spooner, S. J. *J. Appl. Crystallogr.* 1980, 13, 259.
- (20) Hendricks, R. W.; Schelten, J.; Schmatz, W. *Philos. Mag.* 1974, 30, 1974.
- (21) We express our gratitude to M. Zinbo of the Ford Motor Co., who performed the gel permeation analysis.
- (22) The partial specific volume of polystyrene in toluene has been measured by several groups whose results are largely in agreement. Some results are given by: Scholte, Th. G. *J. Polym. Sci.* 1972, A2, 519. Griffel M.; Jessup, R. S.; Cogliano, J. A.; Park, R. P. *J. Res. Natl. Bur. Stand. (U.S.)* 1954, 52, 217. Heller W.; Thompson, A. G. *J. Colloid Sci.* 1951, 6, 54.
- (23) Zimm, B. H. *J. Chem. Phys.* 1948, 16, 1093, 1099.
- (24) Debye, P. J. *J. Phys. Colloid. Chem.* 1947, 51, 18.
- (25) We are grateful for access to a Simplex program copyrighted by J. P. Chandler, Indiana University, Bloomington, IN, 1965.
- (26) Witten, T. A.; Schaefer, L. *J. Chem. Phys.* 1981, 74, 2582.
- (27) Ohta, T.; Oono, Y.; Freed, K. F. *Phys. Rev. A* 1982, 25, 2801.
- (28) Ptitsyn, O. B. *Zh. Fiz. Khim.* 1957, 31, 1091. See also: Hyde, A. J.; Ryan, J. H.; Wall, F. T.; Schatzki, T. F. *J. Polym. Sci.* 1958, 33, 129.
- (29) Greschner, G. S. *Macromol. Chem.* 1973, 170, 203.
- (30) Flory, P. J. *J. Chem. Phys.* 1949, 17, 303.
- (31) Edwards, S. F. *Proc. Phys. Soc.* 1965, 85, 613.
- (32) LeGuillou, J. C.; Zinn-Justin *Phys. Rev. Lett.* 1977, 39, 35.
- (33) Einaga, Y.; Miyake, Y.; Fujita, H. *J. Polymer Sci., Polymer Phys. Ed.* 1979, 17, 2103.
- (34) Weill, G.; des Cloizeaux, J. *J. Phys. (Paris)* 1979, 40, 99.
- (35) Akcasu, A. Z.; Han, C. C. *Macromolecules* 1979, 12, 276.
- (36) Ullman, R. *Macromolecules* 1980, 14, 746.
- (37) Graessley, W. W. *Polymer* 1980, 21, 258.
- (38) Cotton, J. P.; Farnoux, B.; Jannink, G. *J. Chem. Phys.* 1972, 57, 290.
- (39) Benoit, H.; Picot, C. *Pure Appl. Chem.* 1966, 12, 545.
- (40) Wiltzius, P.; Haller, H. R.; Cannell, D. S.; Schaefer, D. W. *Phys. Rev. Lett.* 1983, 51, 1183.
- (41) Domb, C.; Barrett, A. J. *Polymer* 1976, 17, 179.
- (42) Schaefer, D. W. *Polymer* 1984, 25, 387.

Dielectric Relaxation of the Crystal-Amorphous Interphase in Poly(vinylidene fluoride) and Its Blends with Poly(methyl methacrylate)

Bernd Hahn and Joachim Wendorff

Deutsches Kunststoff Institut, D-6100 Darmstadt, West Germany

Do Y. Yoon*

IBM Research Laboratory, San Jose, California 95193. Received August 6, 1984

ABSTRACT: The temperature of the dielectric β -transition of poly(vinylidene fluoride) (PVDF), which is generally assigned to the glass temperature of the liquidlike amorphous phase of PVDF, is found to remain invariant in its compatible blends with poly(methyl methacrylate) (PMMA) in which PVDF exhibits crystallinity. This invariance of the β -transition temperature over a large composition range from PVDF homopolymer to 60/40 PVDF/PMMA and its disappearance in the completely amorphous blends are explicable by recognizing the crystal-amorphous interphase associated with lamellar crystallites of PVDF. These experimental results therefore provide a compelling argument that the β -transition is not related to the liquidlike amorphous phase, but rather arises from the crystal-amorphous interphase in lamellar PVDF crystallites, where PMMA is completely excluded despite favorable segmental (mixing) interactions. The latter point derives from recent theoretical considerations which show that the interphase in lamellar semicrystalline polymers is necessitated by the difficulty in abruptly dissipating the high chain flux at the crystal surface to the level commensurate with the isotropy of the amorphous phase; the presence of PMMA in the interphase will therefore be deleterious in resolving the chain flux problem. It follows then that the strong β -transition of PVDF is indicative of a significant fraction of the interphase region in semicrystalline PVDF, which can be attributed to the presence of considerable amounts of head-to-head and tail-to-tail defects in PVDF chains according to the theory. Relevance of this interphase to dielectric constants and electric-field-induced orientation characteristics of PVDF are also discussed.

Introduction

It is now well established that poly(vinylidene fluoride) (PVDF) and poly(methyl methacrylate) (PMMA) are completely compatible,¹⁻⁴ or miscible, over the entire composition range in the melt below the lower critical solution temperature (LCST) at $\sim 330^\circ\text{C}$.⁵ This has been demonstrated, for example, by the measurements of the Flory-Huggins interaction parameter χ by various methods and the measurements of correlation lengths of concentration fluctuations by the small-angle X-ray scattering (SAXS) method. Upon cooling from the melt, the mixtures containing PVDF fractions less than 50% normally form a completely amorphous phase. In the amorphous blends the complete miscibility of the two polymers is manifested by the continuous change of the "glass temperature" with composition.^{3,6}

The mixtures containing PVDF fractions more than 50% tend to exhibit crystallinity of PVDF below $\sim 170^\circ\text{C}$. Mechanical relaxation measurements of these semicrystalline PVDF/PMMA blends show two transition temperatures with the upper transition occurring around 60°C and the other around -40°C (at 110 Hz).^{3,6} The former corresponds to the glass temperature of the amorphous phase comprising approximately 50/50 PVDF/PMMA, whereas the latter occurs at temperatures very close to the β -transition of PVDF homopolymer.^{3,6}

According to the conclusions of previous studies on the relaxation mechanisms of PVDF,^{7,8} the β -transition is generally believed to arise from the segmental motions in the liquidlike amorphous phase of semicrystalline PVDF and thus is related to its glass temperature. Hence, the fact that this β -transition is changed only slightly upon